International Journal of Modern Physics B
Vol. 17, No. 28 (2003) 4965–4974

World Scientific
www.worldscientific.com

EXCHANGE FREQUENCIES IN THE 2D WIGNER CRYSTAL

B. BERNU* and P. GIANINETTI

Laboratoire de Physique Théorique des Liquides, UMR 7600 of CNRS, Université P. et M. Curie, boite 121, 4 Place Jussieu, 75252 Paris, France
**bernu@lptl.jussieu.fr*

LADIR CÂNDIDO

Instituto de Física de São Carlos, Universidade de São Paulo, 13560-970 São Carlos, SP, Brazil

D. M. CEPERLEY

Dept. of Physics and NCSA University of Illinois at Urbana-Champaign, Urbana, IL 61801, USA

Received 13 July 2001

Path Integral Monte Carlo is used to calculate exchange frequencies as electrons undergo ring exchanges in a "clean" $2d$ Wigner crystal as a function of density. Agreement with WKB calculations is found at very low density, but the results show an enhanced increase with density near melting. Remarkably, the exchange Hamiltonian closely resembles the measured exchanges in $2d$ ^{3}He. Using the resulting multi-spin exchange model we find the spin Hamiltonian for $r_s \geq 175 \pm 10$ is a frustrated antiferromagnetic, with a spin liquid ground state. For lower density the ground state will be ferromagnetic. Some effects of a magnetic field are presented.

1. Introduction

Electrons confined at the surface of helium[1] or at the interface of semiconductor MOSFET's and heterostructures[2] can solidify at low densities. At low temperature, electrons can exchange their positions by tunnelling, a phenomena responsible for the thermodynamics and magnetic properties. In this paper we report on the calculation of exchange frequencies, show how they compare with ^{3}He (already published in Ref. 3) and sketch the main effect of a magnetic field at low density using exact diagonalisation.

The homogeneous $2d$ electron system is characterized by two parameters: the density given in terms of $r_s = a/a_0 = (m^*/m\epsilon)(\pi a_0^2 \rho)^{-1/2}$ and the energy in effective Rydbergs $Ry^* = (m^*/m_e\epsilon^2)Ry$ where m^* is the effective mass and ϵ the dielectric constant. At low density (large r_s) the potential energy dominates over the kinetic energy and the system forms a perfect triangular lattice, the Wigner

crystal.[4] At zero temperature, melting occurs at $r_s \simeq 37 \pm 5$.[5] Classical melting appears at $r_s \geq 100$ for temperatures $T_{\rm melt} = 2Ry^*/(\Gamma_c r_s)$ where $\Gamma_c \approx 137$.[6]

For the perfect solid (no point defects), according to Thouless's theory, the low temperature physics is described by the effective multi-spin exchange (MSE) Hamiltonian:[7]

$$\mathcal{H}_{\rm spin} = -\sum_P (-1)^P J_P \hat{\mathcal{P}}_{\rm spin} \tag{1}$$

where the sum is over all cyclic (ring) exchanges described by a cyclic permutation P, J_P is its exchange frequency and $\hat{\mathcal{P}}_{\rm spin}$ is the corresponding spin exchange operator. As suggested by Thouless[7] and Roger,[8] Path Integral Monte Carlo (PIMC) is a reliable way to calculate these parameters.[9–11] In bulk ^{3}He as well as $2d$ ^{3}He adsorbed on surfaces, it is found that 3, 4, ... ring exchanges are also important.[9–12] In addition, the exchange energies vary rapidly with the density. Thus these systems may have magnetic phase transitions by changing the density, the most simplest one being the ferro-antiferromagnetic transition. When the four or larger loop exchanges are no longer negligible such as close to the melting transition, Néel Long Range Order antiferromagnetic phases may be destroyed by quantum fluctuations. Even if the electrons are in a solid phase, one can have exotic phases such as a spin liquid.

2. The WKB Limit

At large r_s, WKB calculations predicted the three body exchange dominates, thus leading to a ferromagnetic ground state.[8,14] In the WKB method, one keeps only the most probable path, giving the main density dependence of the exchange energy:[8,14]

$$J_P = A_P b_P^{1/2} r_s^{-5/4} e^{-b_P r_s^{1/2}} \tag{2}$$

where $b_P r_s^{1/2}$ is the minimum value of the action integral along the exchanging path. As the 3-particle exchange exponent is the smallest, J_3 dominates at large r_s (see Table 1).

Table 1. WKB $2d$ Wigner crystal parameters of Eq. (2): P is the cycle length of the exchange, b_p the exponent and A_P the prefactor from Ref. 19.

P	b_P	A_P
2	1.644	2.07
3	1.526	0.87
4	1.662	0.99
5	1.911	1.26
6	1.783	1.16
6b	2.134	

3. Path Integral Method

When the temperature is lowered, the electron crystal attains its ground state and the low energy phonons are frozen. Each electron still has a zero point motion with a substantial kinetic energy. When one continues to decrease the temperature, electrons start to exchange their positions by tunnelling, resulting in a spin exchange. Because exchanges are very rare, each exchange can be studied independently. Suppose we label the particles. There are $N!$ such labelling. Starting with a given numbering, one chooses a given permutation P. In the phase space, we denote by Z the position of the original numbering and PZ the position of the permuted system. We are left here with a two-well problem in a multi dimensional space. In this two well system the ground state ψ_0 of energy E_0 is symmetrical and the first excited state ψ_1 of energy E_1 is anti-symmetrical. Other states have much higher energies. The diagonal density matrix element $\langle Z|\exp(-\beta H)|Z\rangle$ and the off-diagonal density matrix element $\langle Z|\exp(-\beta H)|PZ\rangle$ can be expanded as:

$$\langle Z|\exp(-\beta H)|Z\rangle = \psi_0^2(Z)e^{-\beta E_0} + \psi_1^2(Z)e^{-\beta E_1} + \cdots \tag{3}$$

$$\langle Z|\exp(-\beta H)|PZ\rangle = \psi_0(Z)\psi_0(PZ)e^{-\beta E_0} + \psi_1(Z)\psi_1(PZ)e^{-\beta E_1} + \cdots \tag{4}$$

$$= \psi_0^2(Z)e^{-\beta E_0} - \psi_1^2(Z)e^{-\beta E_1} + \cdots \tag{5}$$

where we have used the symmetry properties of the first two states. The ratio of these two density matrix elements is then:

$$F_P(\beta) = \frac{\langle Z|\exp(-\beta H)|PZ\rangle}{\langle Z|\exp(-\beta H)|Z\rangle} = \tanh(J_P(\beta - \beta_0))\,, \tag{6}$$

where J_P is the exchange frequency and $\beta_0 = \ln[\psi_1(Z)/\psi_0(Z)]$. Because $J_P\beta \gg 1$, one linearises the previous equation and the slope of $F_P(\beta)$ gives the exchange energy. In terms of path integrals, one interprets $F_P(\beta)$ as the free energy necessary to make an exchange beginning with one arrangement of particles to lattice sites Z and ending on a permuted arrangement PZ. More details can be found in Refs. 3, 9–11.

Figure 1 shows the probability of presence of particle in the xy plane during exchanging paths. The first neighbours of exchangers must move away in order to give space to exchange paths (in particular, see the 2 body exchange). In this figures the most important exchanges are represented. Larger cycles as well as exchanges including second neighbour will have significantly smaller contributions.

4. Results and Comparison with ^{3}He

Results for $r_s \geq 50$ are published in Ref. 3. In these calculations all particles were distinguishable particles. We have found that exchange processes destabilise the solid of distinguishable particles for $r_s < 45$. In order to stabilise the solid, we use Fermi statistics on the non-exchanging particles. The simplest thing to do is to suppose a ferromagnetic ordering of the non exchanging particles. We have

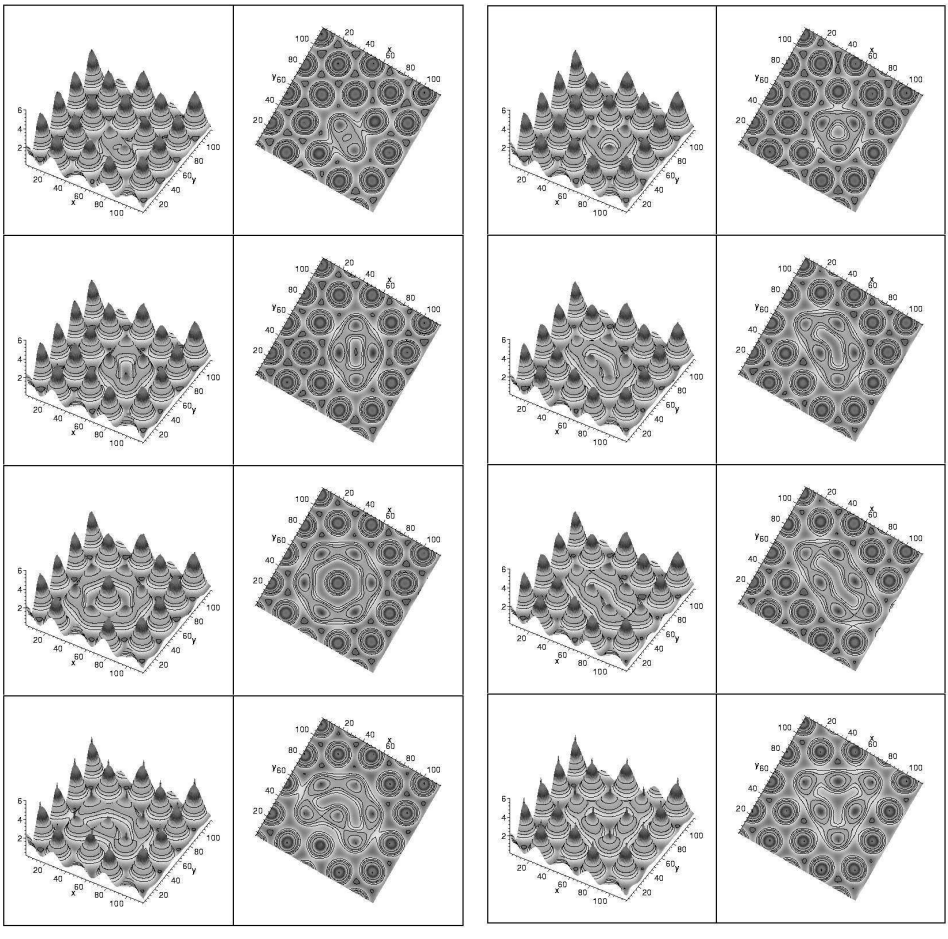

Fig. 1. 3d plot of the one body density probability during exchanging paths at $r_s = 40$, each data are represented from the side and from the top. The top 8 figures show 2, 3, 4 and 5 body exchanges, while the bottom 8 figures show the various 6 body exchanges. The "cones" represent the non exchanging particles. Notice that the centre of mass of first neighbours of the exchanging particles are displaced from lattice position and their sizes are shrunken, especially in the 2 body exchange case. Note also the low probability density between electrons in the 6 body exchanges of the last row, indicating that those exchanges will be less probable.

obtained converged exchange energies for $r_s \geq 35$, a value close to the melting transition.[15]

The WKB approximation suggests plotting the exchange energies versus $r_s^{1/2}$ as shown in Fig. 2. The two body exchange becomes larger than the 3 body one for $r_s < 100$. Except close to the melting transition, all exchange energies are much less than the zero point energy of the electron, thus justifying the use of Thouless' theory. As the variations are almost linear in Fig. 2, the WKB method captures most of the density dependency. Nevertheless, as we will see in the next section, small

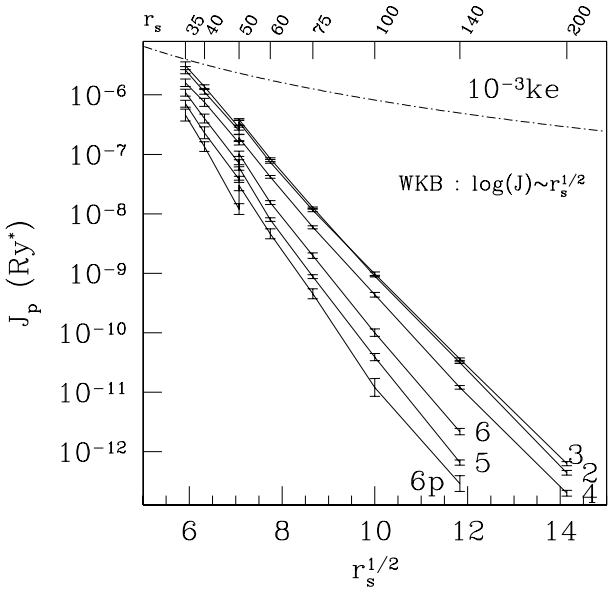

Fig. 2. Exchange energies versus $r_s^{1/2}$. For $r_s \geq 50$ non-exchanging electrons are distinguishable, and for $r_s \leq 50$, there are polarised (preliminary results). One can see that near melting, exchange energies become comparable with the kinetic energy.

deviations from the WKB approximation are enough to provide strong shifts in the transitions. Also, as we approach the melting transition ($r_s \sim 35$), the exchange energies become much more similar to each other.

5. The Magnetic Phase Diagram

The same form of MSE Hamiltonian is obtained for various spin systems. Indeed, a pure triangular solid is found at least for two experimental realisations: ^{3}He adsorbed on graphite and the Wigner crystal. Even if the absolute exchange energies are very different in both cases, only the relative exchange values are relevant to determine the magnetic ground state. Indeed, one can scale all energies by picking up one of the exchanges. For spin 1/2 systems, J_2 and J_3 contribute only with a nearest neighbour Heisenberg term: $J_2^{\text{eff}} = J_2 - 2J_3$, that parameter can be positive or negative and thus is not suitable for scaling the energy. Thus we use J_4 as a reference to fix the overall scale of the magnetic energy. Keeping the most important parameters, the Hamiltonian still has 3 remaining parameters J_2^{eff}/J_4, J_5/J_4 and J_{6h}/J_4 (hexagonal exchange). This Hamiltonian has a non trivial ground state (see Fig. 3).[16] The shape of the ferromagnetic(F)–antiferromagnetic(AF) transition can be easily understood keeping in mind the alternative effects of the even and odd permutations. J_2^{eff} gives a F ground state if negative and an AF ground state if positive. A J_4 (AF coupling) pushes this transition to negative values $J_2^{\text{eff}}/J_4 \sim -4.5$. In the AF region, increasing J_5 will cross the $F - AF$ transition. Finally,

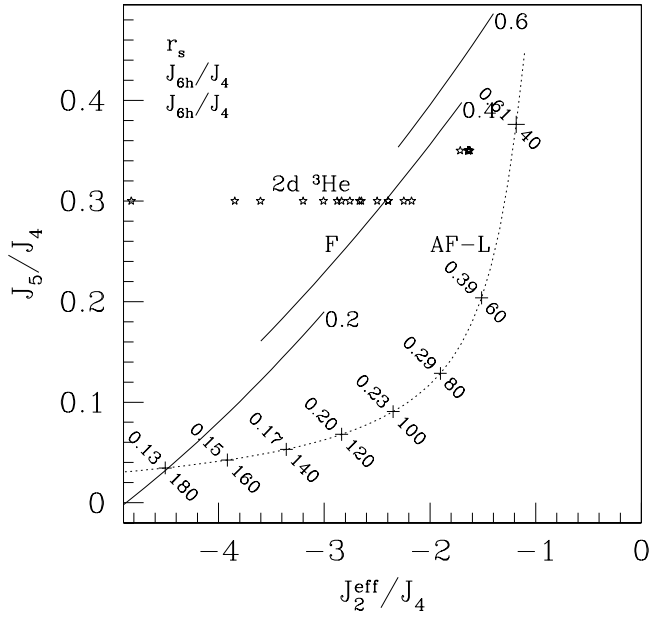

Fig. 3. Zero temperature magnetic phase diagram of the MSE Hamiltonian.[16]

any J_6 will displace the transition line towards the F region. The lines have been obtained from exact diagonalisation.[16]

When we report our data on this diagram (see Fig. 3), we estimate the $F - AF$ transition to occur at $r_s = 175 \pm 10$. At higher density, the frustration between large cyclic exchanges (4-6 body loops) results in a disordered spin state.[16] For example, the point ($J_2^{\text{eff}}/J_4 = -2$, $J_5 = 0$, $J_{6h} = 0$), close to the parameters at $r_s = 100$, is a spin liquid with a gap to all excitations.[16] Near melting, the trajectory approaches again the $F - AF$ transition line, with the possibility of a re-entrant ferromagnetic phase.

In the same figure the exchange parameters extrapolated from measurements of the second layer of ^{3}He absorbed on graphite are reported.[17] It is remarkable to see that they are very similar to the present study, in particular when approaching the melting transition. Yet the interactions of these two systems are very different from a short range strongly repulsive potential for helium to a long range smooth potential for electrons. The search of an underlying universal mechanism is thus highly desirable (possibly the virtual vacancy-interstitial (VI) mechanism).[12]

6. Effect of the Magnetic Field

When electrons exchange their position, they encircle an area. In presence of an external magnetic field ($B_\perp$) perpendicular to the solid, a complex phase factor

modifies the exchange constant:[18]

$$\mathcal{H} = \sum_{\langle i,j \rangle} J_2 P_{ij} - \sum_{\langle ijk \rangle} J_3 (e^{i\phi_3} P_{ijk} + e^{-i\phi_3} P_{ijk}^{-1}) + \sum_{\langle ijkl \rangle} J_4 (e^{i\phi_4} P_{ijkl} + e^{-i\phi_4} P_{ijkl}^{-1}) + \cdots \tag{7}$$

where $\phi_i = 2\pi i e B_\perp a_p / h$, and we have neglected the Zeeman term. a_p is the area of the exchanges given roughly by the formula $a_p = (k+1)a_t$, with a_t the triangle area and k is is number of triangles in the exchange. (This was determined during the PIMC calculation.) Note that no phase factor is associated with the two-body exchange. For electrons, the area is proportional to r_s^2 and reasonable magnetic field may drive phase transitions. Recent WKB evaluations of exchange energies have been done.[19]

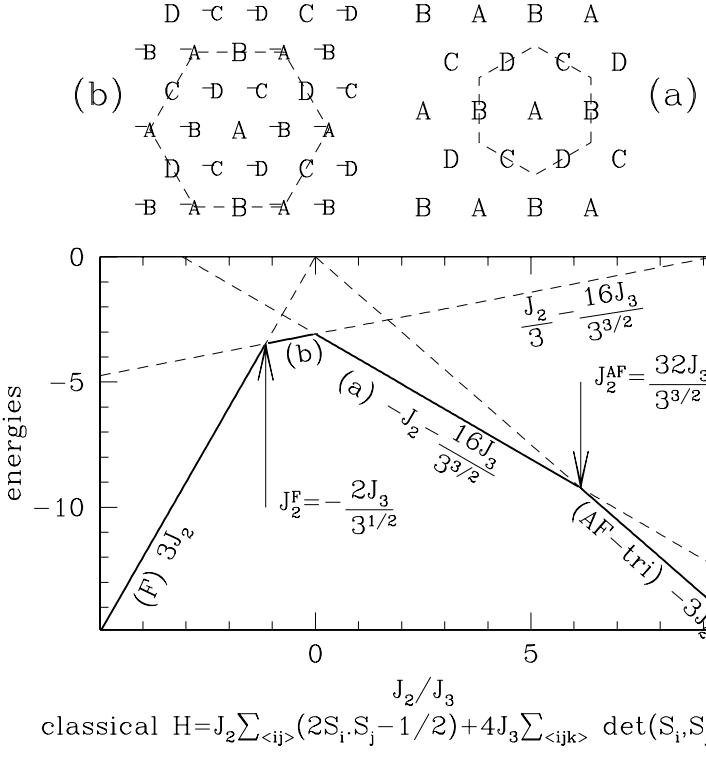

Fig. 4. Top: Possible ground states of the pure chiral classical Hamiltonian on the triangular lattice: (a) the cell has four sites; (b) the cell has twelve sites. Each letter (A, B, C or D) correspond to a given orientation (with the condition $A + B + C + D = 0$) and the minus sign means the opposite orientation. Bottom: ground state energy of the $J_2 - J_3$ classical Hamiltonian versus J_2/J_3. The energy of each state ((A), (B), F and AF) is reported.

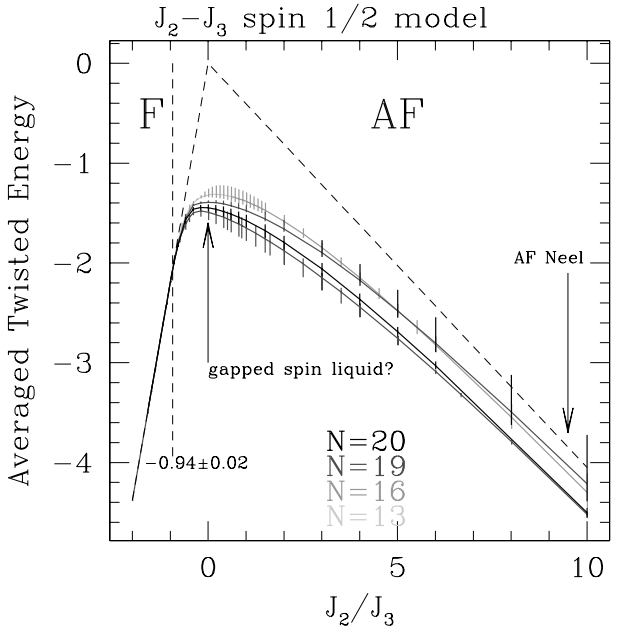

Fig. 5. Ground state energy of the quantum spin 1/2 chiral Hamiltonian of Eq. (8) versus J_2/J_3. The dashed lines are the ferromagnetic and antiferromagnetic energies of the Heisenberg model on the triangular lattice. The vertical dashed line is the estimated $F - AF$ transition value. The full line are the averaged energies, whereas the small vertical line indicate the minimum and maximum energies due to twisted boundary conditions.

Keeping only the 2 and 3 body permutations, the dominant terms at low density, one rewrites Eq. (7) as

$$\mathcal{H} = \sum_{\langle i,j \rangle} J_2^{\text{eff}} P_{i,j} + \sum_{\langle ijk \rangle} J_3^{\text{eff}} i(P_{ijk} - P_{ijk}^{-1}) \tag{8}$$

where $J_2^{\text{eff}} = (J_2 - 2J_3 \cos(\phi_3))$ and $J_3^{\text{eff}} = J_3 \sin(\phi_3)$. Note that the last term in Eq. (8) is a pure chiral term. Here, we show preliminary results on the phase diagram of this Hamiltonian.[20] We see that $J_2^{\text{eff}}/J_3^{\text{eff}}$ takes all possible positive and negative values when the magnetic field varies. Figure 4 shows the phases in the classical limit: i) a ferromagnetic phase at large negative J_2/J_3; ii) three antiferromagnetic Néel Long Range Order phases with successively 4, 12 and 3 sublattices when J_2 increases; iii) all these transitions are first order.

Exact diagonalisations have been done on small samples ($N \leq 20$). For each size, we have computed the ground state energy for twisted boundary conditions and averaged over it (see Fig. 5). The $F - AF$ transition value is estimated at $J_2/J_3 = -0.94 \pm 0.02$, a larger value than the classical one. In the intermediate region (J_2/J_3 between -0.94 and 6), no signature of Néel Long Range Order has been found. On the contrary, evidence of a spin liquid with gap is seen. Quantum fluctuations, as it is often the case, destroy classical Néel Long Range Order when

it has more than 3 sublattices. For instance, we are not able to locate the transition between the AF spin liquid phase and the Néel Long Range Order phase that exists at large J_2/J_3.

7. Conclusions

We have computed several exchange energies by path integral Monte Carlo for the homogeneous Wigner crystal. The importance of more than the 2 and 3 body exchange is crucial to determine the magnetic ordering of the ground state. We found a ferromagnetic ground state for $r_s > 200$ and an antiferromagnetic spin liquid for lower r_s. Surprisingly, the relative exchange energies near melting are very similar to those obtained for a solid layer of ^{3}He adsorbed on graphite, suggesting a possible universal behaviour of the exchange mechanism near the melting transition.

The magnetic order will be very sensitive to a magnetic field, as electron are far away from each other. Indeed a transverse magnetic field can induce $F - AF$ transitions that can help to determine precise values of exchange energies. As the Hamiltonian in a magnetic field contains chiral terms, "exotic" phases can be observed in the AF region.

Acknowledgments

This research was funded by NSF DMR 98-02373, the CNRS-University of Illinois exchange agreement, support by Fundação de Amparo à Pesquisa do Estado de São Paulo (FAPESP) and the Dept. of Physics at the University of Illinois. We used the computational facilities at the NCSA.

References

1. C. C. Grimes and G. Adams, *Phys. Rev. Lett.* **42**, 795 (1979).
2. J. Yoon *et al.*, *Phys. Rev. Lett.* **82**, 1744 (1999).
3. B. Bernu, L. Candido and D. Ceperley, *Phys. Rev. Lett.* **86**, 870 (2001).
4. X. Zhu and S. G. Louie, *Phys. Rev.* **B52**, 5863 (1995).
5. B. Tanatar and D. M. Ceperley, *Phys. Rev.* **B39**, 5005 (1989).
6. K. Strandburg, *Rev. Mod. Phys.* **60**, 161 (1988).
7. D. J. Thouless, *Proc. Roy. Soc.* **A86**, 893 (1965).
8. M. Roger, *Phys. Rev.* **B30**, 6432 (1984).
9. D. M. Ceperley, *Rev. Mod. Phys.* **67**, 279 (1995).
10. D. M. Ceperley and G. Jacucci, *Phys. Rev. Lett.* **58**, 1648 (1987).
11. B. Bernu and D. Ceperley, in *Quantum Monte Carlo Methods in Physics and Chemistry*, eds. M. P. Nightingale and C. J. Umrigar (Kluwer, 1999).
12. M. Roger, J. H. Hetherington and J. M. Delrieu, *Rev. Mod. Phys.* **55**, 1 (1983).
13. K. Voelker and S. Chakravarty, cond-mat/0107151.
14. M. Katano and D. S. Hirashima, *Phys. Rev.* **B62**, 2573 (2000).
15. B. Bernu, L. Candido and D. Ceperley, to be published.
16. G. Misguich, B. Bernu, C. Lhuillier and C. Waldtmann, *Phys. Rev. Lett.* **81**, 1098 (1998); *Phys. Rev.* **B60**, 1064 (1999).

17. M. Roger, C. Bauerle, Yu. M. Bunke, A.-S. Chen and H. Godfrin, *Phys. Rev. Lett.* **80**, 1308 (1998).
18. S. A. Kivelson *et al.*, *Phys. Rev.* **B36**, 1620 (1987); T. Okamoto and S. Kawaji, *Phys. Rev.* **B57**, 9097 (1998).
19. K. Voelker and S. Chakravarty, cond-mat/0107151.
20. B. Bernu and P. Gianinetti, to be published.